



Catalytic conversion of substituted and un-substituted cyclohexanone into corresponding enones and phenols by nanocatalysts under acid or base-free reaction conditions

Mazloom Shah ^{a,b,*}, Fan Zhang ^{a,c}, Ashfaq Ahmad ^b

^a Key Laboratory of Tropical Plant Resources and Sustainable Use, Biomass Group, Xishuangbanna Tropical Botanical Garden Chinese Academy of Science, Kunming 650223, PR China

^b Department of Chemistry, Women University of Azad Jammu and Kashmir, Bagh 12500, Pakistan

^c University of Chinese Academy of Sciences, Beijing, 100049, China



ARTICLE INFO

Article history:

Received 6 September 2016

Received in revised form 12 October 2016

Accepted 30 October 2016

Available online 1 November 2016

Keywords:

Metallic and bimetallic nanoparticles

Heterogeneous nanocatalysts

Catalytic conversion

Cyclic ketones

Enones and phenols

ABSTRACT

The catalytic conversion of substituted and unsubstituted cyclohexanones to the corresponding enones and aromatic alcohol catalyzed by Pd, Pd-1, Pd-cube, Cu, Ni, Ag@Pd and Ni-Sn nanocatalysts has been studied in the presence of O₂ as the oxidant without using any additives i.e. acid or base or ligand. The optimization of experimental parameters for dehydrogenation of cyclohexanones was established to achieve maximum yield of the product by using Pd nanocatalyst. The conversion of cyclohexanone, cyclohexenone, 3-methyl cyclohexanone and 3-methyl cyclohexenone catalyzed by Pd nanocatalyst at 80 °C, 10 atm O₂ pressure after 24 h, led to a 79%, 49%, 62% and 25% yields of desired products, respectively. Then, the conversion of substituted and unsubstituted cyclohexanones investigated in the presence of various nanocatalysts i.e., Pd-1, Pd-cube, Cu, Ni, Ag@Pd and Ni-Sn nanoparticles and was compared their percentage yields.

© 2016 Elsevier B.V. All rights reserved.

1. Introduction

The conversion of cyclic ketones into corresponding aromatic alcohol is a fundamental reaction in organic chemistry. Phenols and its derivatives are versatile synthetic intermediates due to their application in the preparation of polymers, pharmaceuticals, dyes and bulk chemicals [1]. In this regard, a variety of methods and catalyst system have been well documented for the catalytic dehydrogenative aromatization of ketones to aromatic alcohol, however, these protocols use undesirable stoichiometric reagents such as DDQ (2,3-dichloro-5,6-dicyano-1,4-benzoquinone), use stepwise procedures such as bromination/dehydrobromination, low product yields, require harsh reaction conditions, limited access to starting materials, and formation of isomeric products [2–16]. The dehydrogenation of cyclic ketone affords corresponding cyclic-enone or aromatic alcohol via removal of 1 or 2 equivalent of H₂, respectively. Hirao et al. represented oxidative aromatization of a variety of substituted cyclohexanones catalyzed

by NH₄VO₃ or VOSO₄ with Bu₄NBr/HBr and trifluoroacetic acid (TFA) as additives [5]. Recently, the group of Stahl reported a Pd-based homogeneous catalyst system using O₂ as the terminal oxidant for the dehydrogenative aromatization of substituted cyclohexanones in the presence of *p*-toluenesulfonic acid and 2-(*N,N*-dimethylamino)pyridine. More recently, a thorough investigation of the Pd (TFA)₂/2-Me₂Npy-catalyzed dehydrogenation of cyclohexanones and cyclohexenones, showing that an initial, highly active molecular Pd (II) species generate soluble Pd nanoparticles that serve as the active catalyst during steady-state dehydrogenation of the substrate [17–19]. In contrast, no effective heterogeneous catalytic method for aromatization of substituted and unsubstituted cyclic ketones exist. The advantage of a heterogeneous catalyst lies in its easy separation from the reaction mixture by simple filtration and possibility to be recycled several times.

Here we report the conversion of cyclohexanone to the corresponding cyclohexenone and phenol catalyzed by Pd, Pd-1, Pd-cube, Cu, Ni, Ag@Pd and Ni-Sn nanocatalyst in the presence of O₂ as the oxidant without using any additives i.e. ligand or acid or base. The effect of various parameters such as catalyst concentration, solvent, temperature, O₂ pressure and reaction time on catalytic conversion of cyclohexanone to the cyclohexenone and phenol has also been investigated. Furthermore, Pd nanocatalyst was

* Corresponding author at: Department of Chemistry, Women University of Azad Jammu and Kashmir, Bagh 12500, Pakistan.

E-mail address: shahmazloom@yahoo.com (M. Shah).

tested for conversion of cyclohexenone, 3-methyl cyclohexanone and 3-methyl cyclohexenone at optimized reaction conditions for cyclohexanone.

2. Experimental

2.1. Materials

L-ascorbic acid ($C_6H_8O_6$), palladium acetate ($Pd(CH_3COO)_2$), potassium bromide (KBr), sodium borohydride ($NaBH_4$), ethylene glycol ($HOCH_2CH_2OH$), polyvinylpyrrolidone with an average molecular weight of 10,000 (PVP), acetone (CH_3COCH_3), ethanol (C_2H_5OH), cyclohexanone ($C_6H_{10}O$), cyclohexenone (C_6H_8O), 3-methylphenol ($CH_3C_6H_4(OH)$), toluene ($C_6H_5CH_3$), ethyl acetate ($CH_3COC_2H_5$), acetic acid (CH_3COOH), dimethylformamide ($(CH_3)_2NC(O)H$), dimethylacetamide ($CH_3C(O)N(CH_3)_2$), 1-methyl-2-pyrrolidinone (C_5H_9NO) were purchased from Sino-pharm chemical reagent Co. Ltd., palladium nitrate hydrate ($Pd(NO_3)_2 \cdot 2H_2O$) from Aladdin, Sodium tetrachloropalladate ($Na_2PdCl_4 \cdot nH_2O$) from Shanxi kaida chemical engineering Co. Ltd., Sodium sulfate (Na_2SO_4) from Shanghai rich joint chemical reagent Co. Ltd., 3-methyl cyclohexanone ($CH_3C_6H_9O$) from Tokyo chemical industry Co. Ltd., copper acetate monohydrate ($Cu(CH_3COO)_2 \cdot H_2O$) from Shanghai chemical reagent company, *p*-anisaldehyde from Aladdin chemistry Co. Ltd., 3-methyl cyclohexenone ($CH_3C_6H_7O$) from Energy chemical and silver nitrate ($AgNO_3$) and nickel (II) formate dihydrate ($Ni(HCOO)_2 \cdot 2H_2O$) from Alfa Aesar.

2.2. Nanocatalysts preparation

2.2.1. Pd, pd-1 and Ag@Pd coreshell nanoparticles preparation

Pd (Pd-PVP), Pd-1 (Pd-oleylamine) and Ag@Pd coreshell nanoparticles were prepared per guidelines reported previously [20,21]. For Pd-1 nanoparticles preparation, 0.424 g oleic acid and 0.401 g oleylamine were put in 50 ml ethylene glycol. Next, metal-precursor solutions, 0.5 mmol Pd ($CH_3COO)_2$ in acetone was added. The reaction mixture was heated at 393 K for 30 min under vigorous stirring. Subsequently, the temperature was raised to 473 K and kept at reflux for 60 min. The nanoparticles were separated from the mixture through extraction with *n*-hexane.

2.2.2. Pd-cube nanoparticles preparation

In case of Pd-cube nanoparticles [22], calculated amount of poly(vinyl pyrrolidone) (PVP), L-ascorbic acid (60 mg), KBr (300 mg) and Na_2PdCl_4 (57 mg) were dissolved in 11 ml of water. The resulting solution was heated at 353 K in air under magnetic stirring for 3 h and then cooled to room temperature. Nanoparticles were collected by centrifugation and then washed four times with a water-acetone mixture.

2.2.3. Ni, Cu and Ni-Sn nanoparticles preparation

For preparation of Ni nanoparticle 0.24 g $Ni(HCOO)_2 \cdot 2H_2O$ and calculated amount of PVP were dissolved in 35 ml of ethylene glycol and the solution was heated to 342 K while stirring until the formation of a completely homogeneous blue solution. Once at this temperature, 0.15 g of $NaBH_4$ was added under magnetic stirring. The resultant solution was refluxed at 468 K for 2.5 h [23]. In case of Cu nanoparticle preparation calculated amount of $Cu(CH_3COO)_2 \cdot H_2O$ and PVP were added in 70 ml of ethylene glycol and the solution was heated to 323 K while stirring until the formation of a completely homogeneous solution. Once at this temperature, 0.34 g of $NaBH_4$ was added under magnetic stirring. The resultant solution was refluxed at 463 K for 2.5 h. In case of Ni-Sn nanoparticle preparation calculated amount of $Ni(HCOO)_2 \cdot 2H_2O$, $SnCl_2 \cdot 2H_2O$ and PVP were added in 35 ml of ethylene glycol and the solution was

heated to 323 K while stirring until the formation of a completely homogeneous blue solution. At 323 K, 0.18 g of $NaBH_4$ added under magnetic stirring and resultant solution was refluxed at 471 K for 2.5 h. The nanoparticles were precipitated in acetone, washed with acetone, ethanol and dried in air at room temperature.

2.3. Catalytic reaction of substituted and un-substituted cyclohexanones

In catalytic reaction, catalyst (2.8–5.1 mol%), cyclohexanones (0.5 mmol), DMSO (0.5 ml) and stir bar were added to a 10 ml schlenk tube. O_2 was bubbled through the solution for 10 min at room temperature. The reaction was heated in an oil bath to 80 °C with vigorous stirring under a balloon of O_2 for given time. After the completion of the reaction, the reaction mixture was filtered.

In case of using high pressure reactor, catalyst (2.8–5.1 mol%), the substituted or un-substituted cyclohexanones (0.5 mmol) and DMSO (1 ml) were placed in a reactor. After purging the pressure reactor with O_2 , the reactor was loaded with given O_2 pressure (25 °C). The reaction was heated to 80 °C with vigorous stirring for given time. After the completion of the reaction, the reaction mixture was filtered. Then, the residue was extracted with ethyl acetate. The products were identified with GC-MS and quantified by GC analysis.

2.4. Instrumentation

The crystalline nature of the materials prepared was determined by X-Ray Diffraction (XRD) using a Rigaku TTR-III diffractometer operated at 200 mA and 40 kV with a monochromated $Cu K\alpha$ radiation ($\lambda = 1.541 \text{ \AA}$) – step size = 0.02, time per step = 10 or 20 s/step, the scan rate was 8°/min. The average crystallite size of nanoparticle was calculated from XRD using Scherrer equation: $L = K\lambda/\beta\cos\theta$, where L is the average crystallite size, K is the Scherrer constant related to the shape and index (hkl) of the crystals, λ is the wavelength (0.15406 nm) of the X-rays, β is the additional broadening (in radians) and θ is the Bragg angle, respectively. SEM studies were performed on a JSM-6700F scanning electron microscope. TEM analyses were performed on a JEM-2011 transmission electron microscope operating at 200 kV. The microstructure and chemical composition of the bimetallic nanoparticles were analyzed by using a High-resolution transmission electron microscope (HR-TEM) (JEM-2010) which was operated at the accelerating voltage of 300 keV, equipped with EDS. GC-MS analyses were performed by using a Thermo Finnigan Trace GC coupled to MS IS2 MSD. Gas chromatographic analysis of reactions was conducted with a Shimadzu GC-17A gas chromatograph with a DB-Wax column.

3. Result and discussion

3.1. Nano-catalysts characterization

The synthesis conditions used for the preparation of metallic Pd, Pd-1, Pd cube, Cu and Ni nanoparticles and bimetallic Ag@Pd, and Ni-Sn nanoparticles are summarized in Table 1. Nanoparticles were evaluated by powder X-ray diffraction (XRD), scanning electron microscope (SEM), transmission electron microscopy (TEM) and energy dispersive X-ray analysis (EDX). SEM, TEM and EDX were used to analyze morphology and elemental composition of nanoparticles while Nanoparticles crystal phases were identified by XRD. XRD patterns of Pd before and after reaction, Pd-1, Cu, Pd-cube, Ni, Ni-Sn and Ag@Pd nanoparticles are shown in Fig. 1(d) and Fig. 3(c). Four diffraction peaks at $2\theta = 39.21, 45.87, 68.11$ and 82.07° correspond to the (111), (200), (220) and (311) crystal planes of metallic Pd [24,25], confirming the formation of Pd nanoparticles. The diffraction peaks in XRD pattern of Ag@Pd nanoparticles

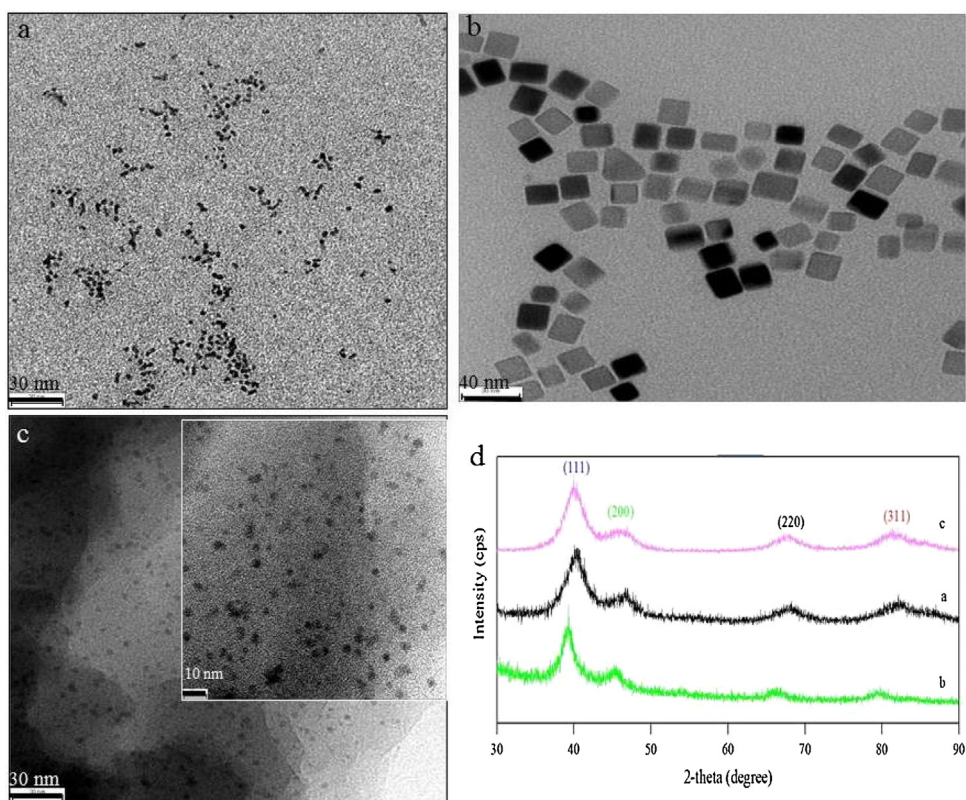


Fig. 1. (a) (b) and (c) are TEM images of Pd nanoparticles, Pd cube and Pd nanoparticles after reaction (d) Powder XRD patterns of a = Pd-1, b = Pd and C = Pd after reaction.

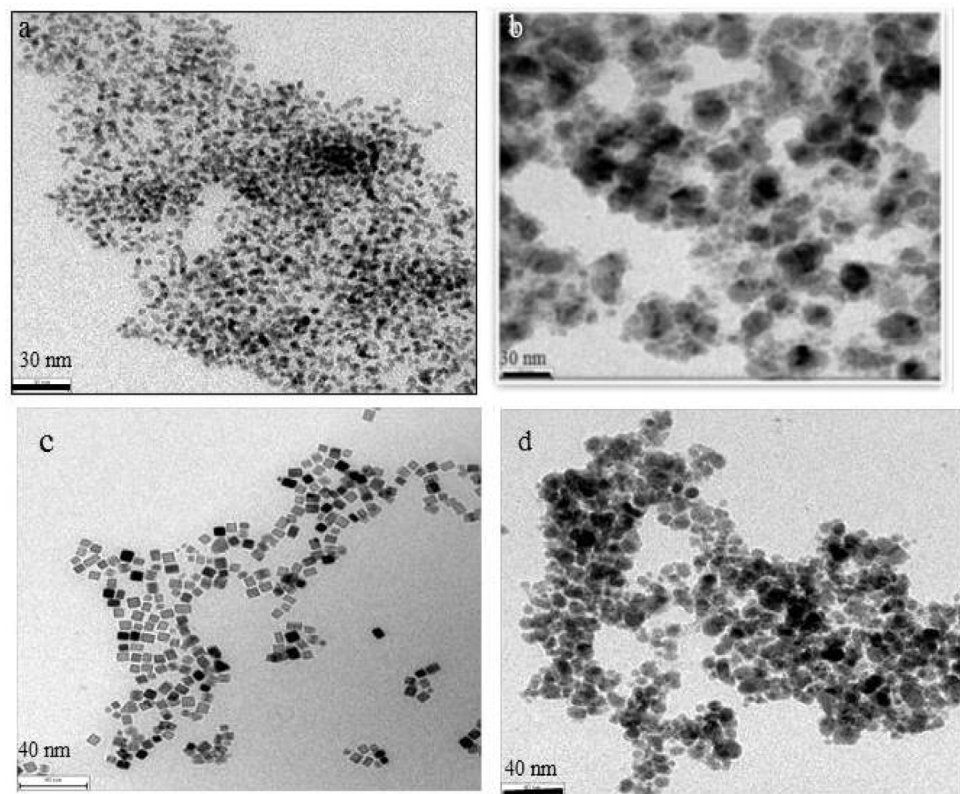
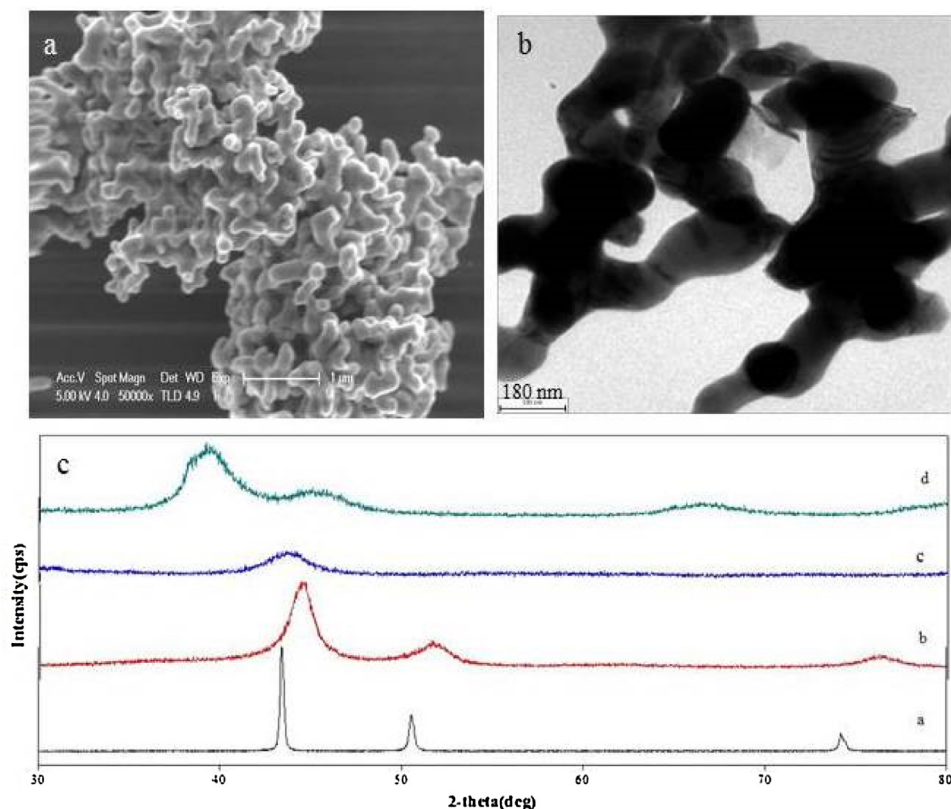


Fig. 2. (a) (b), (c) and (d) the TEM images of Pd-1, Ni, Pd-cube and Ni-Sn nanoparticles respectively.

Table 1

Reaction conditions for nanoparticles preparation.

Nanoparticles	Precursors (mol l ⁻¹)	Reaction solvent	Protecting agents	Reducing agents	T (°C)	Reaction Time (min)
Pd	Palladium(II) nitrate hydrate (0.0016)	Ethylene glycol	PVP	—	120	120
Ag@Pd	Palladium(II) nitrate hydrate (0.0016) Silver(II) nitrate (0.023)	Ethylene glycol	PVP	—	90	120
Pd-1	Palladium(II) acetate (0.0005)	Ethylene glycol	Oleylamine	—	200	120
Pd-cube	Sodium tetrachloropalladate	Water	PVP	L-ascorbic acid	80	180
Ni	Nickel (II) formate dihydrate (0.03)	Ethylene glycol	PVP	NaBH ₄	195	150
Ni-Sn	Nickel (II) formate dihydrate (0.03) Tin (II) chloride dihydrate (0.01)	Ethylene glycol	PVP	NaBH ₄	198	150
Cu	Copper (II) acetate monohydrate (0.037)	Ethylene glycol	PVP	NaBH ₄	190	150

**Fig. 3.** (a) and (b) SEM and TEM images of Cu nanoparticles respectively, (c) Powder XRD patterns of a = Cu, b = Ni, c = Ni-Sn and d = Ag@Pd nanoparticles.

progressively shifted to higher intensity and lower 2θ values without forming any discrete Ag and Pd reflections which showed the bimetallic nature of the nanoparticles, as opposed to a physical mixture of separately nucleated monometallic Pd and Ag particles (Fig. 3c-d). Three peaks at $2\theta = 44.38, 51.67$, and 76.57° correspond to the (111), (200) and (220) crystal planes of metallic Ni, confirming the formation of pure face-centered-cubic Ni nanoparticles (Fig. 3c-b). Diffraction patterns of bimetallic Ni-Sn nanoparticles show a crystalline structure, where two broad diffraction lines at 30.41° and 43.05° clearly observed were similar to previous work [23]. The broadening of peaks in the X-ray diffraction patterns is because of very small crystallite size [26–28]. Fig. 3c-a shows, three sharp peaks at 2θ values of $43.39^\circ, 50.56^\circ$, and 74.24° , correspond-

ing to (111), (200), and (220) planes of metallic copper [29–31] while no impurity peaks such as CuO , Cu_2O , or $\text{Cu}(\text{OH})_2$ were found in the X-ray diffraction pattern.

Representative TEM images of the as-prepared, Pd, Pd-1, Pd-cube, Ni, Cu and Ni-Sn, nanoparticles are shown in Figs. 1 a, 2 a, 1 b and 2 c, 2 b, 3 b and 2 d, respectively. The average particle sizes of the Pd nanoparticles were obtained around 3.1 nm with spherical morphology. The mean diameter of the nanoparticles was calculated from counting about 100 metal particles. Metallic Ni and bimetallic Ni-Sn nanoparticles were observed to have a mixture of irregular shape and spherical morphology with an estimated average size of 13 nm and 8 nm, respectively (Fig. 2b and d). EDX analysis of the Ni-Sn nanoparticles indicated that Sn concentration on

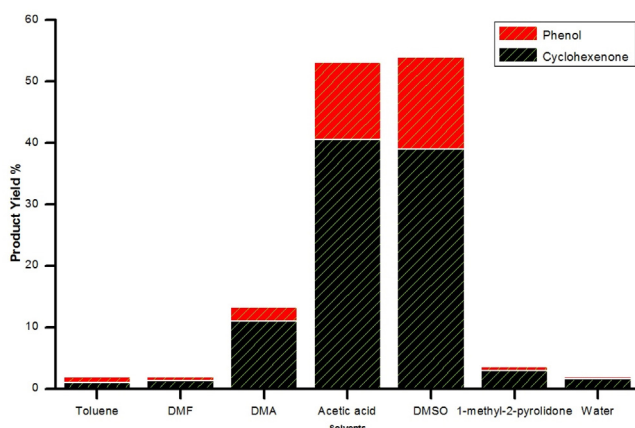


Fig. 4. Solvents screening for the catalytic conversion of cyclohexanone. Reaction conditions; substrate 0.5 mmol, 3.8 w.t% Pd nanocatalyst, 1 atm O₂ pressure, 80 °C, 24 h

the agglomerated particles was higher than on the well dispersed nanoparticles. The Pd-cube nanoparticles were cubic shapes with average diameters of 7 nm (Fig. 2c). While the Cu nanoparticles were irregular shapes with average diameters of 98 nm (Fig. 3a–b). Although the Cu nanoparticles were encapsulated with a PVP capping layer, the agglomeration behavior observed among them is astonishing. The sticky surface characteristics of Cu nanoparticles covered with PVP cause aggregation of the nanoparticles during drying.

3.2. Catalytic conversion of cyclohexanones to corresponding cyclohexenone and phenol catalyzed by Pd nanocatalyst

Our initial studies targeted the identification of optimized reaction conditions for catalytic conversion of cyclohexanone to cyclohexenone and phenol by Pd nanocatalyst. The catalytic conversion of cyclohexanone to the corresponding aromatic alcohol catalyzed by Pd nanocatalyst without using additives, in the presence of O₂ as the oxidant was investigated. The criterion for the optimization was the selection of parameters such as solvent, catalyst concentration, temperature, O₂ pressure and reaction time which produce maximum desired product yield. Aiming to ultimately assess the solvent effects on the aerobic dehydrogenation of cyclohexanone, we first explored the influence of several solvents in the reaction. Fig. 4 summarizes the results from the catalytic conversion of cyclohexanone with Pd nanoparticles conducted in several solvents at 80 °C under 1 atm O₂ (RT) for 24 h. The results in Fig. 4 reveal that the reaction depends heavily upon the nature of solvent. Among different solvents tested, Pd showed the best performance in DMSO.

Variability in O₂ pressure (1–10 atm), reaction temperature (60–100 °C), catalyst dosage (2.5–5.1 wt%) and reaction time (60–1800 min) were studied for the conversion of cyclohexanone to cyclohexenone and phenol catalyzed by Pd nanocatalyst (Fig. 5).

The effect of O₂ pressure on the conversion of cyclohexanone to cyclohexenone and phenol was checked in the range of 1–10 atm using 2.5 wt.% Pd as catalyst at 80 °C for 24 h and the results depicts that the %age yield of phenol increases with the increase in O₂ and was maximum at 10 atm (Fig. 5a). When the oxygen pressure was increased from 1 to 5 atm the product yield jumped sharply from 54% to 74% and reached the highest value of 75% at 10 atm. The dehydrogenation of cyclohexanone at low O₂ pressure favors formation of cyclohexenone; whereas at high O₂ pressure promotes highly selective formation of phenol. Therefore, 10 atm pressure of O₂ was selected for further investigations.

The effect of the reaction temperature on the catalytic conversion of cyclohexanone into cyclohexenone and phenol was investigated using 2.5 wt.% Pd as catalyst, O₂ pressure of 10 atm and reaction time of 24 h. The reaction temperature was varied from 60 to 100 °C at an interval of 10 °C. The product yield sharply increased from 19.50% to the highest value of 75% as temperature grew from 60 to 80 °C and gradually decreased to 47% and 38.90% at 90 and 100 °C (Fig. 5b). Therefore, in this work, the best temperature is chosen as 80 °C.

The Pd nanocatalyst concentration was increased from 0.9 to 5.1 wt% for the conversion of cyclohexanone into cyclohexenone and phenol under conditions of 10 atm oxygen pressure, reaction temperature of 80 °C and reaction time of 24 h. The yield jumped sharply from 23% to 75% as catalyst rose from 0.9 to 3.8 wt%, and reached the highest value of 79% at 5.1 wt% catalyst (Fig. 5c). Catalyst of 5.1 wt% with the highest product yield of 79% is selected as the best value for the next optimization.

Reaction time from 1 to 30 h was chosen for catalytic conversion of cyclohexanone into cyclohexenone and phenol under conditions of 5.1 wt% catalyst, 10 atm oxygen pressure and reaction temperature of 80 °C (Fig. 5d). When time rose from 1 to 24 h, product yield increased from 1.4% to 79% sharply, and gradually rose to 82% at 30 h. Since little increased for product yield from 24 to 30 h, the best value for reaction time is selected as 24 h.

3.3. Catalytic conversion of cyclohexenone, 3-methyl cyclohexanone and 3-methyl cyclohexenone to corresponding phenol catalyzed by Pd nanocatalyst

Then, Pd nanocatalyst was tested for the conversion of cyclohexenone, 3-methyl cyclohexanone and 3-methyl cyclohexenone to the corresponding phenols under the best reaction conditions of cyclohexanone dehydrogenation i.e., 5.1w.t% catalyst, 80 °C temperature, 10 atm O₂ pressure, dimethylsulfoxide (DMSO) as the solvent and 24 h reaction time. The results show that the performance of the same catalyst under same reaction conditions for different substrates is different. The conversion of cyclohexanone, cyclohexenone, 3-methyl cyclohexanone and 3-methyl cyclohexenone into corresponding aromatic alcohols catalyzed by Pd nanocatalyst, led to a 79%, 49%, 62% and 25% yields of desired product, respectively (Table 2).

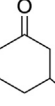
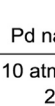
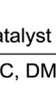
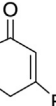
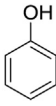
3.4. Catalytic conversion of cyclohexanones to corresponding cyclohexenone and phenol catalyzed by different nanocatalysts

Furthermore, the catalytic conversion of cyclohexanone to the corresponding cyclohexenone and phenol catalyzed by different nanocatalysts in the presence of O₂ as the oxidant was investigated. The conversion of cyclohexanone and 3-methylcyclohexanone with Pd, Pd-1, Pd-cube, Cu, Ni, Ni-Sn, and Ag@Pd nanoparticles conducted in dimethylsulfoxide (DMSO) as the solvents under 10 atm O₂ (RT) at 80 °C for 24 h (Table 3). The metallic Pd nanoparticles exhibited excellent catalytic performance as compared with Pd-1, Pd-cube, Ni, Ni-Sn, Cu and Ag@Pd nanoparticles under mild reaction conditions. The conversion of cyclohexanone in the absence of catalyst was quite slow resulted in no conversions after 24 h (Table 3, Entry 1). The order of activity at 80 °C temperature was Pd > Pd-1 > Pd-cube > Ni > Ni-Sn, > Ag@Pd > Cu nanocatalyst in dimethylsulfoxide (DMSO). The high catalytic activity of Pd nanocatalyst is because of having small crystallite size, small particle size and high surface area as compared to Pd-1 and Pd-cube nanocatalysts. The addition of Ag to Pd and Sn to Ni failed to enhance the catalytic activity of Pd and Ni nanoparticles, respectively (Table 3, entries 2–4, 12–15, 10–11).

In the view of industrial purposes, reusability of the Pd nanocatalyst was investigated for the conversion of cyclohexanone to

Table 2

Catalytic conversion of cyclic ketones catalyzed by Pd nanocatalyst.

Entry	Reagent	Nano-catalyst (wt.%)	P (atm)	Time h	Yield (%)		Product Yield%
					Cyclic enone (2)	Phenol (3)	
1		No Catalyst	1	24	0	0	0
3		Pd (3.8)	1	24	39	15	54
4		Pd(3.8)	5	24	25	49	74
5		Pd(5.1)	10	24	23	56	79
7		Pd(3.8)	1	24	—	24	24
9		Pd(3.8)	10	24	—	46	46
		Pd(5.1)	10	24	—	49	49
10		Pd(3.8)	1	24	1.0	35	36
11		Pd(3.8)	5	24	2	37	39
		Pd(5.1)	10	24	8	54	62
12		Pd(3.8)	1	24	—	19	19
13		Pd(3.8)	10	24	—	22	22
14		Pd(5.1)	10	24	—	25	25

Reaction conditions; substrate 0.5 mmol, 5.1 w.t.% nanocatalyst, 10 atm O₂ pressure, 80 °C, 24 h. Yield were determined by using *p*-anisaldehyde as internal standard.**Table 3**

Catalyst optimization for catalytic conversion of cyclic ketones.

Entry	Nano-catalyst (wt.%)	T (°C)	P (atm)	Time h	Yield (%)		Product Yield%
					Cyclic enone (2)	Phenol (3)	
1	No catalyst	80	1	24	—	—	0
2	Pd (3.8)	80	1	24	39	15	54
3	Pd (3.8)	80	10	24	20	55	75
4*	Pd (3.8)	80	10	24	6	53	59
5	Pd-1(3.8)	80	10	24	9	36	45
6	Pd-cube(3.8)	80	10	24	20	4	24
7	Cu (3.8)	80	1	24	0.2	0.8	1
8	Cu (3.8)	80	10	24	0.5	4.5	5
9*	Cu (3.8)	80	1	24	0	2	2
10	Ni (3.8)	80	10	24	0	23	23
11	Ni-Sn (3.8)	80	10	24	0.5	13.3	13.8
12	Ag-Pd (3.8)	80	1	24	15.4	2.3	17.7
13	Ag-Pd (3.8)	80	10	24	0.5	8	8.5
14*	Ag-Pd (3.8)	80	1	24	2	3	5
15*	Ag-Pd (3.8)	80	10	24	20	10	30

Reaction conditions; substrate 0.5 mmol (For * R = CH₃ and others R = H), 3.8 w.t.% nanocatalyst, 10 atm O₂ pressure, 80 °C, 24 h. Yield were determined by using *p*-anisaldehyde as internal standard.**Table 4**

The catalyst reusability for catalytic conversion of cyclohexanone.

Cycle	Nano-catalyst (wt.%)	Time h	Yield (%)		Product Yield%
			Cyclohexenone (2)	Phenol (3)	
1	Pd (3.8)	24	20	55	75
2	Pd (3.8)	24	20	55	75
3	Pd (3.8)	24	19.5	54	73.5

Reaction conditions; substrate 0.5 mmol cyclohexanone, 3.8 w.t.% Pd nanocatalyst, 10 atm O₂ pressure, 80 °C, 24 h. Yield were determined by using *p*-anisaldehyde as internal standard.

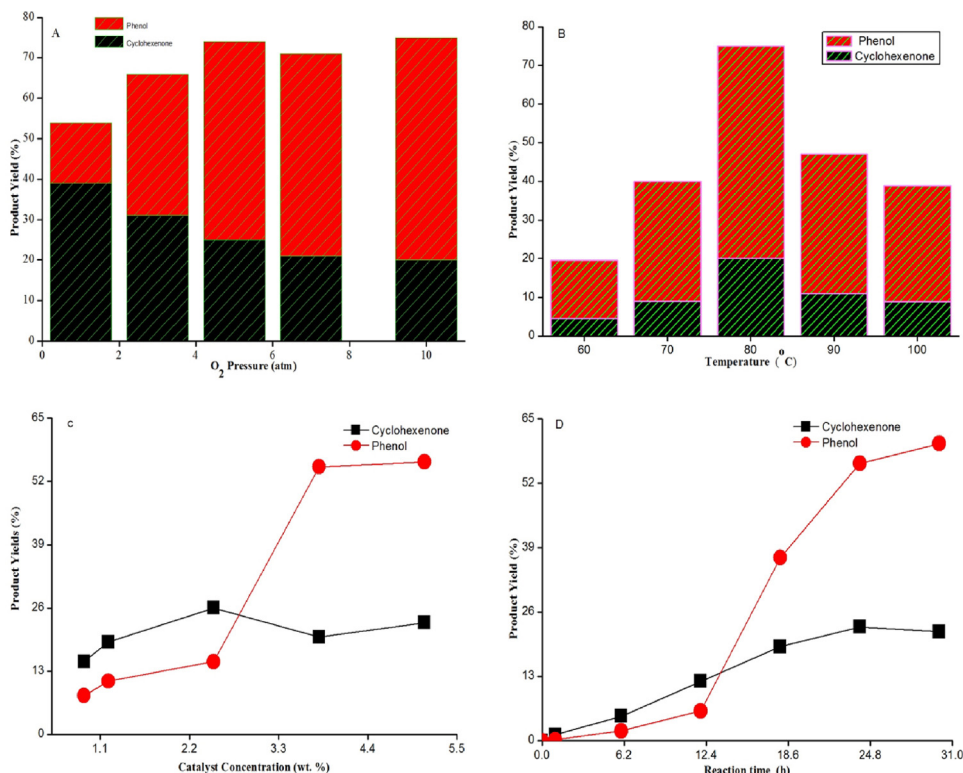


Fig. 5. Optimization of different reaction conditions (A) O₂ pressure, (B) Reaction temperature, (C) Catalyst concentration and (D) Reaction time for the catalytic conversion of cyclohexanone to corresponding cyclohexenone and phenol catalyzed by heterogeneous Pd nanocatalyst.

corresponding cyclohexenone and phenol, by carrying out repeated runs (1–3 cycles) of the reaction on the same batch of the catalyst. In order to regenerate the catalyst, after each run, it was separated by a filtration, washed several times with acetone, deionized water and ethyl acetate. Then, it was dried under vacuum at room temperature and reused in the subsequent run. The catalyst can be reused for 1–2 cycles without any significant loss of activity (Table 4). There was only a slight deactivation when third trial of the Pd nanocatalyst was conducted but the reason of catalyst deactivation is not yet known. It is speculated that there was little loss of nanocatalyst during testing and washings. TEM and XRD results confirmed that there is no change in morphology, particle size and XRD pattern of the Pd nanoparticle after reaction (Fig. 1a,c,d).

4. Conclusions

The catalytic conversion of substituted and unsubstituted cyclohexanones to the corresponding phenols catalyzed by various nanocatalysts in the presence of O₂ as oxidant without using any additives (acid or base) was investigated. The catalytic conversion of cyclohexanone catalyzed by Pd, Pd-1, Pd-cube, Ni, Ni-Sn, Cu and Ag@Pd nanocatalyst (3.8 wt%) at 80 °C, 10 atm O₂ pressure after 24 h, led to a 75%, 45%, 23%, 24%, 13.8%, 5% and 8.5% yields of desired product, respectively. Among different nanocatalysts, Pd nanocatalyst showed the best performance. The maximum yield of 82% was achieved for the catalytic conversion of cyclohexanone catalyzed by Pd nanocatalyst (5.1 wt%), at 80 °C, 10 atm O₂ pressure after 30 h. The dehydrogenation of cyclohexanone at low O₂ (1 atm) pressure favors formation of cyclohexenone; whereas at high O₂ (10 atm) pressure promotes highly selective formation of phenol. Furthermore, transmission electron microscopy (TEM) and X-ray diffraction (XRD) confirmed that there was no change in morphology, crystal phases and particles size of Pd nanocatalyst after the reaction.

Acknowledgements

This work was supported by higher education commission of Pakistan (21-791/SRG/R&D/HEC2016). M. Shah is also grateful for a generous XTBG-CAS postdoctoral fellowship.

References

- [1] J.H.P. Tyman, *Synthetic and Natural Phenols*, Vol. 52, Elsevier, Amsterdam, 1996.
- [2] P. Bamfield, P.F. Gordon, *Chem. Soc. Rev.* 13 (1984) 441.
- [3] E.C. Horning, M.G. Horning, *J. Am. Chem. Soc.* 69 (1947) 1359.
- [4] P.P. Fu, R.G. Harvey, *Chem. Rev.* 78 (1978) 317.
- [5] T. Moriuchi, K. Kikushima, T. Kajikawa, T. Hirao, *Tetrahedron Lett.* 50 (2009) 7385.
- [6] C.Y. Yi, D.W. Lee, *Organometallics* 28 (2009) 947.
- [7] P.F. Schuda, W.A. Price, *J. Org. Chem.* 52 (1987) 1972.
- [8] J. Muzart, J.P. Pete, *J. Mol. Catal.* 15 (1982) 373.
- [9] T.T. Wenzel, *J. Chem. Soc. Chem. Commun.* 1989 (1989) 932.
- [10] M. Hayashi, K. Yamada, S. Nakayama, *Perkin Trans. 1* (2000) 1501–1503.
- [11] S. Kamiguchi, S. Nishida, M. Kodomari, T. Chihara, *J. Cluster Sci.* 16 (2005) 77–91.
- [12] C.S. Yi, D.W. Lee, *Organometallics* 28 (2009) 947–949.
- [13] T. Hirao, M. Mori, Y.J. Ohshiro, *Organ. Chem.* 55 (1990) 358–360.
- [14] T. Hirao, M. Mori, Y. Ohshiro, *Chem. Lett.* 20 (1991) 783–784.
- [15] J. Muzart, *Eur. J. Org. Chem.* 2010 (2010) 3779.
- [16] D.R. Buckle, *Encyclopedia of Reagents for Organic Synthesis*, in: D. Crich (Ed.), Wiley, New York, 2010.
- [17] Y. Izawa, D. Pun, S.S. Stahl, *Science* 333 (2011) 209–213.
- [18] D. Pun, T. Diao, S.S. Stahl, *J. Am. Chem. Soc.* 135 (2013) 8213–8221.
- [19] T. Diao, D. Pun, S.S. Stahl, *J. Am. Chem. Soc.* 135 (2013) 8205–8212.
- [20] K. Tedsee, T. Li, S. Jones, C.W.A. Chan, K.M.K. Yu, P.A.J. Bagot, E.A. Marquis, J.D.W. Smith, S.C.E. Tsang, *Nat. Nanotechnol.* 6 (2011) 302–307.
- [21] Z. Yin, W. Zhou, Y. Gao, D. Ma, C.J. Kiely, X. Bao, *Chemistry* 18 (2012) 4887–4893.
- [22] G. Li, H. Kobayashi, J.M. Taylor, R. Ikeda, Y. Kubota, K. Kato, M. Takata, Y. Yamamoto, S. Toh, S. Matsumura, H. Kitagawa, *Nat. Mater.* 13 (2014) 803–806.
- [23] M. Shah, Q.X. Guo, Y. Fu, *Catal. Commun.* 65 (2015) 85–90.
- [24] L.J. Chen, C.C. Wan, Y.Y. Wang, *J. Colloid Interface Sci.* 297 (2006) 143–150.
- [25] Z. Yin, Y. Zhang, K. Chen, J. Li, W. Li, P. Tang, H. Zhao, Q. Zhu, X. Bao, D. Ma, *Nat. Sci. Rep.* (2016), <http://dx.doi.org/10.1038/srep04288>.

- [26] G.G. Couto, J.J. Klein, W.H. Schreiner, D.H. Mosca, A.J.A. De Oliveira, A.G. Zarbin, *J. Colloid Interface Sci.* 311 (2007) 461–468.
- [27] M. Niederberger, M.H. Bartl, G.D. Stucky, *Chem. Mater.* 14 (2002) 4364–4370.
- [28] T. Ungar, *Scr. Mater.* 51 (2004) 777–781.
- [29] B.K. Park, S. Jeong, D. Kim, J. Moon, S. Lim, J. Sub Kim, *J. Colloid Interface Sci.* 311 (2007) 417–424.
- [30] K.J. Carroll, J.U. Reveles, M.D. Shultz, S.N. Khanna, E.E. Carpenter, *J. Phys. Chem. C* 115 (2011) 2656–2664.
- [31] Y. Jianfeng, Z. Guisheng, Hu. Anming, Y.N. Zhou, *J. Mater. Chem.* 21 (2011) 15981–15986.